

# GNN-based Path-aware multi-view Circuit Learning for Technology Mapping

Wentao Jiang<sup>\*</sup>

Faculty of Electrical Engineering and Computer Science, NingBo University NingBo, China

Jingxin Wang<sup>\*</sup>

University of Michigan-Shanghai Jiao Tong University Joint Institute, Shanghai Jiao Tong University ShangHai, China

Zhang Hu

Faculty of Electrical Engineering and Computer Science, NingBo University NingBo, China

Zhengyuan Shi

Department of Computer Science and Engineering, The Chinese University of Hong Kong Hong Kong, China

Chengyu Ma

Faculty of Electrical Engineering and Computer Science, NingBo University NingBo, China

Qiang Xu

Department of Computer Science and Engineering, The Chinese University of Hong Kong Hong Kong, China

Weikang Qian

University of Michigan-Shanghai Jiao Tong University Joint Institute, Shanghai Jiao Tong University ShangHai, China

Zhufei Chu<sup>†</sup>

Faculty of Electrical Engineering and Computer Science, NingBo University NingBo, China

## Abstract

Traditional technology mapping suffers from systemic inaccuracies in delay estimation due to its reliance on abstract, technology-agnostic delay models that fail to capture the nuanced timing behavior of real post-mapping circuits. To address this fundamental limitation, we introduce GPA (graph neural network (GNN)-based Path-Aware multi-view circuit learning), a novel GNN framework that learns precise, data-driven delay predictions by synergistically fusing three complementary views of circuit structure: And-Inverter Graphs (AIGs)-based functional encoding, post-mapping technology-specific encoding, and path-aware Transformer pooling that dynamically emphasizes critical timing paths. Trained exclusively on real cell delays extracted from critical paths of industrial-grade post-mapping netlists, GPA learns to classify cut delays with unprecedented accuracy, directly informing smarter mapping decisions. Evaluated on the 19 EPFL combinational benchmarks, GPA achieves 19.9%, 2.1%, and 4.1% average delay reduction over conventional heuristic methods (techmap, MCH) and the prior state-of-the-art ML-based approach SLAP, respectively—without compromising area efficiency.

1 2

## 1 Introduction

As a pivotal stage in logic synthesis, technology mapping transforms a technology-independent Boolean network into a functionally equivalent, gate-level netlist compliant with a target standard-cell library. The quality of the mapped design is ultimately assessed through static timing analysis (STA) and area estimation, with the primary objective being to minimize critical-path delay while optimizing area overhead. Effective mapping thus requires

balancing these competing metrics to achieve high-performance, silicon-efficient implementations.

To enhance technology mapping outcomes, techniques such as structural choice [1, 2], heterogeneous logic representations (e.g., MIGs) [3], and extensive technology-independent optimizations are widely employed as preprocessing steps. These methods aim to enrich the structural diversity and algebraic expressiveness of the input network, thereby expanding the solution space for subsequent mapping. However, they remain fundamentally technology-independent: while area can be reliably determined from library specifications, delay estimation relies on abstract, pre-characterized models that are decoupled from post-mapping circuit context [4]. As a result, critical dependencies such as load capacitance, signal transition, and path correlation are ignored during optimization, leading to significant mismatches between predicted and actual delays—a key impediment to achieving timing-closed synthesis.

As illustrated in the motivating example of Figure 1, we perform ten random shuffles of the cut sets at each node to perturb the selection order during delay-oriented mapping. The resulting mappings reveal significant performance variation, with the default mapping engine outcome (marked by the red star) yielding the worst critical-path delay and offering no improvement in Area-Delay Product (ADP) compared to several alternative selections (denoted by green circles). Notably, even in this small-scale circuit, the baseline method fails to consistently identify the optimal cut configuration—highlighting the sensitivity of mapping outcomes to heuristic ordering and the absence of accurate, context-aware delay estimation.

<sup>1\*</sup>These authors contributed equally to this work

<sup>2†</sup>Corresponding author

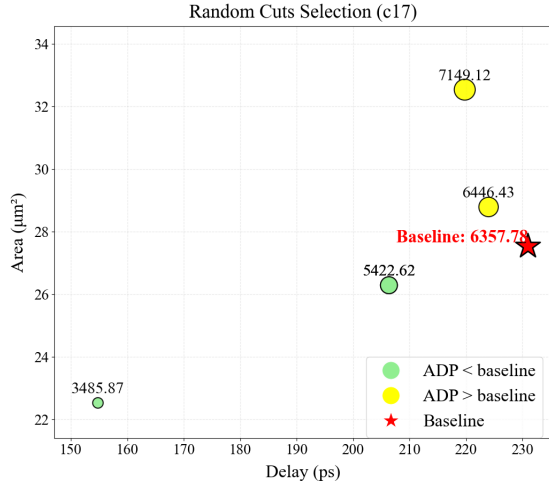


**Figure 1: Experimental Results by Random Cuts Selection**

This experiment underscores a fundamental limitation of traditional approaches: the semantic gap between technology-independent circuit representations and technology-dependent physical realities. Conventional methods lack mechanisms to incorporate post-mapping timing feedback into early-stage decisions, leading to inaccurate delay prediction and, consequently, suboptimal gate binding. As a result, mapping engines remain blind to path-dependent effects, preventing them from achieving truly optimized implementations—even when superior alternatives exist within the same cut space.

Unlike heuristic methods, ML-based approaches like SLAP [5], LEAP [6], and AiMap [7] use handcrafted features to predict cut/ surrogate delays from post-mapping data. Yet their performance is limited by rigid, manually designed representations that fail to capture path-dependent, technology-specific timing behavior—hindering generalization and accuracy.

Accurate delay prediction and cut evaluation require rich functional and structural circuit information, as cell delays are highly sensitive to post-mapping context—such as load, inverter insertion, and pin-specific timing—while cuts are identified via Boolean matching. However, handcrafted features cannot adequately represent unique Boolean functions or capture complex topological relationships. Consequently, they often conflate structurally or functionally distinct sub-circuits, leading to misclassification and poor generalization across diverse circuit instances—severely limiting scalability in real-world mapping flows.

To overcome these limitations, we propose GPA (GNN-based Path-aware multi-view circuit learning for technology mapping), a framework that jointly models functional semantics and structural topology to predict post-mapping cell delays. GPA leverages graph neural networks (GNNs) for circuit-wide propagation and a path-aware Transformer pooling module to generate cut embeddings from leaf nodes, enabling accurate delay estimation grounded in critical-path timing. Trained with logic-1 probability and masked modeling objectives—inspired by [8]—GPA learns expressive node embeddings that capture both Boolean functionality and cross-view

structural context without handcrafted features, thereby enabling precise cut matching as validated in [9].

To validate GPA’s practical impact, we integrate it into ALSO, an open-source logic synthesis framework built on mockturtle, and compare against the established mapping strategies versatile mapping [10] (command `techmap`) and mixed structural choices [2] (command `mch`). During cut generation, GPA infers a delay class for each candidate cut, which is then used to refine node arrival time estimation in the mapping engine. Across the 19 EPFL combinational benchmarks, GPA achieves 19.9% and 2.1% average delay reduction over `techmap` and `mch`, respectively. Moreover, against the prior ML-based state-of-the-art SLAP, GPA demonstrates a 4.1% improvement—validating the effectiveness of its functional and path-aware multi-view learning paradigm.

## 2 Related Work

### 2.1 Circuit Representation Learning

Circuit representation learning seeks to produce expressive embeddings by capturing diverse structural and functional circuit features to support downstream EDA tasks. Pioneered by DeepGate [11], this paradigm uses logic-1 probabilities from random simulation to train node embeddings rich in functional semantics—enabling applications in testability analysis [12], logic equivalence checking [13], and cell-type prediction [9]. Subsequent works, including the DeepGate family [8, 14, 15], HOGA [16], and PolarGate [17], enhance logic-1 probability estimation through advanced architectures and training objectives. However, these methods remain fundamentally technology-independent, focusing primarily on And-Inverter Graph (AIG)-level semantics. As a result, their single-view embeddings cannot encode post-mapping context—such as cell-level timing or load effects—critically limiting their applicability to technology-aware tasks like high-fidelity delay prediction and optimal cut selection in modern mapping flows.

Multi-view learning offers strong potential for EDA, yet current approaches face critical limitations [18, 19]. While recent efforts leverage large language models (LLMs) with textual summaries and netlists to improve Verilog understanding [20, 21], they remain disconnected from practical EDA toolflows, hindering real-world applicability. DeepCell [9] marks a step toward grounded learning by jointly embedding AIGs and post-mapping netlists—the first framework to explicitly learn from technology-mapped circuits. However, its multi-view paradigm is narrowly focused on refining logic-1 probability prediction, without extending to broader synthesis tasks such as delay-aware cut selection or integration into mapping engines. Consequently, the full potential of multi-view learning for technology-aware EDA remains unrealized.

### 2.2 Technology Mapping

As a critical phase in logic synthesis, technology mapping translates technology-independent logic representations—such as AIGs—into optimized, library-based netlists composed of standard cells, adhering to the timing, power, and area constraints of a target fabrication technology [1].

In technology mapping, a cut—a fundamental structural primitive—comprises a root node together with a set of leaf nodes, such that every path from the primary inputs (PIs) to the root traverses

at least one leaf node [22]. During the pre-mapping phase, cuts are constructed in topological order by recursively merging the cuts of child nodes, followed by Boolean matching to identify library-compatible implementations. Each node then selects an optimal cut by estimating its arrival time using pin-based cell delays within a dynamic programming framework. However, this approach inherently assumes that standard-cell delays are context-independent, neglecting the strong influence of path-specific loading, signal correlation, and downstream logic on actual timing behavior. Consequently, the delay estimates often deviate significantly from post-mapping reality, undermining mapping optimality.

Recent advances have sought to enrich logic representations to enhance mapping flexibility and reduce structural bias. Techniques such as those in [1, 23] integrate structural choice networks as optional constructs during logic optimization, enabling more diverse decomposition paths. Concurrently, other works explore alternative algebraic frameworks: for instance, Majority-Inverter Graphs (MIGs) have been leveraged in [3, 24] to enable more efficient logic optimization and improved mapping outcomes through enhanced expressiveness. Building on this direction, MCH [2] combines structural choices with heterogeneous logic representations—such as AIGs and MIGs—to further diversify the solution space and achieve state-of-the-art mapping performance. Despite their advantages, these approaches remain fundamentally technology-independent, relying on abstract cost models that are decoupled from actual circuit timing post-mapping. As a result, they fail to close the critical gap between high-level logic restructuring and technology-specific implementation, limiting their ability to deliver consistently optimal results in physical-performance metrics such as delay and power.

### 3 Methodology

#### 3.1 Overview

As shown in Fig 2, the overview of our proposed framework, GNN-based Path-aware Circuit Learning (GPA). The work flow which GPA is integrated is presented in Fig. 3. The central challenge in technology mapping is the discrepancy between pre-mapping delay estimates and actual post-mapping circuit performance. GPA addresses this by serving as an intelligent guidance mechanism for the mapper.

The workflow proceeds as follows: First, we input the technology-independent And-Inverter Graph (AIG) netlist into a standard logic synthesis tool, which generates a comprehensive set of candidate cuts for each node. Next, our pre-trained GPA model performs inference on these cuts to classify them, predicting their post-mapping delay characteristics. This classification, which is trained on real post-mapping delay data, serves as a highly accurate cost metric. This metric is then used by the mapper’s dynamic programming algorithm to calculate arrival times, allowing it to select an optimal cut for each node based on realistic delay information rather than inaccurate, pre-defined models.

#### 3.2 AIG Encoder

Given an AIG, represented as a graph  $\mathcal{G}^A = (\mathcal{V}^A, \mathcal{E}^A)$ , the AIG encoder  $\Phi^A$  is responsible for learning informative node-level representations. To capture the distinct structural and functional properties of each node  $i \in \mathcal{V}^A$ , the encoder produces two separate embeddings.

Formally, the encoder  $\Phi^A$  generates the complete set of node embeddings  $\mathbf{H}^A = \{H_i^A \mid i \in \mathcal{V}^A\}$  from the graph  $\mathcal{G}^A$ :

$$\mathbf{H}^A = \Phi^A(\mathcal{G}^A) \quad (1)$$

Each individual embedding  $H_i^A$  is a composite of its structural part,  $hs_i^A \in \mathbb{R}^d$  (capturing graph topology), and its functional part,  $hf_i^A \in \mathbb{R}^d$  (capturing the logic operation):

$$H_i^A = \{hs_i^A, hf_i^A\} \quad (2)$$

For use in subsequent modules, these two embeddings are concatenated to form a single initial node representation  $h_i \in \mathbb{R}^{2d}$ :

$$h_i = \text{cat}(hs_i^A, hf_i^A) \quad (3)$$

#### 3.3 Post-mapping Encoder

To make the model aware of the target technology’s physical constraints (e.g., standard cell library properties or FPGA architecture), we employ a Post-Mapping (PM) encoder,  $\Phi^P$ . This encoder, typically implemented as a simple MLP, processes a feature vector  $F_p$  that represents the characteristics of the target technology. It generates a single, global target-aware embedding  $e_p \in \mathbb{R}^{d_p}$ , where  $d_p$  is the dimension of this physical embedding:

$$e_p = \Phi^P(F_p) \quad (4)$$

This embedding  $e_p$  provides global context to the rest of the model.

#### 3.4 Path-aware GAT Transformer Pooling

This module is the core of GPA, responsible for generating a single, predictive embedding  $e_C$  for each candidate cut  $C$  from the initial node embeddings  $h_i$ . This is achieved in a two-step process.

**3.4.1 Path-Aware Contextualization.** First, to capture path-level information and refine the initial node embeddings  $h_i$ , we apply a global Graph Attention (GAT) layer,  $G_p$ . This layer allows each node to aggregate information from its multi-hop neighborhood, producing a path-aware embedding  $z_i \in \mathbb{R}^{2d}$  for each node  $i$ :

$$z_i = G_p(\{h_j \mid j \in \mathcal{V}^A\}, \mathcal{E}^A) \quad (5)$$

where  $\{h_j \mid j \in \mathcal{V}^A\}$  is the set of all concatenated node embeddings and  $\mathcal{E}^A$  is the AIG’s edge set.

**3.4.2 Cut-Level Aggregation.** To generate a single embedding  $e_C$  for a specific candidate cut  $C \subset \mathcal{V}^A$ , we must model the complex interactions \*within\* the cut. We first apply a dedicated cut-transformer,  $\mathcal{T}_C$ , to the set of path-aware embeddings  $\{z_j \mid j \in C\}$  for all nodes belonging to that cut:

$$\{\hat{z}_j \mid j \in C\} = \mathcal{T}_C(\{z_j \mid j \in C\}) \quad (6)$$

This produces a set of contextualized node embeddings  $\{\hat{z}_j\}$  that reflect intra-cut interactions.

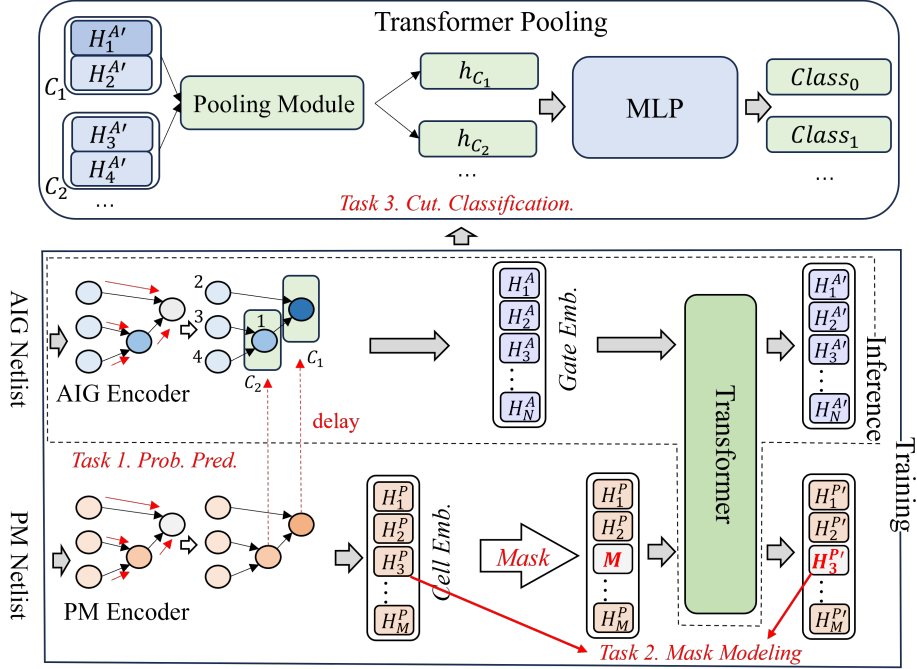


Figure 2: Model overview of GPA: First, the AIG Encoder and PM Encoder extract node embeddings from the logic network and technology-specific constraints, respectively, optimized via structural mask modeling and functional probability prediction tasks. Then, the Path-aware Transformer Pooling module aggregates context from the leaf nodes of a target cut. Finally, an MLP classifier utilizes the generated cut embedding to predict the post-mapping delay class.

Finally, to produce a fixed-size representation for the entire cut, we apply an averaging pooling layer  $P_{\text{avg}}$  to the transformer’s output, yielding the final cut embedding  $e_C \in \mathbb{R}^{2d}$ :

$$e_C = P_{\text{avg}}(\{\hat{z}_j \mid j \in C\}) = \frac{1}{|C|} \sum_{j \in C} \hat{z}_j \quad (7)$$

This embedding  $e_C$ , potentially concatenated with the global technology embedding  $e_p$ , is fed to the final classifier.

### 3.5 Model Pre-training

To endow the AIG encoder  $\Phi^A$  with a general-purpose understanding of circuit structure and function, we pre-train it on the AIG graph  $\mathcal{G}^A$  using a multi-task objective.

**Structural Task:** To train the structural embeddings  $hs_i^A$ , we task the model with predicting masked edges  $(u, v)$  from the graph. The structural embeddings of the two endpoint nodes are concatenated and passed to a classifier  $M_s$ . This objective forces the structural embedding  $hs^A$  to encode connectivity information, and its loss function  $\mathcal{L}_s$  is:

$$\mathcal{L}_s = \sum_{(u, v) \in \mathcal{E}_m^A} \text{BCE}(M_s(\text{cat}(hs_u^A, hs_v^A)), 1) \quad (8)$$

where  $\mathcal{E}_m^A$  is a set of randomly masked edges and BCE denotes the Binary Cross-Entropy loss.

**Functional Task:** To train the functional embeddings  $hf_i^A$ , we predict the logic function (node type)  $y_f^i$  at each node  $i$  (e.g., AND, NOT, or Primary Input) using a classifier  $M_f$ . This objective forces

the functional embedding  $hf^A$  to encode the node’s logic, with the loss  $\mathcal{L}_f$  defined as:

$$\mathcal{L}_f = \sum_{i \in \mathcal{V}^A} \text{CE}(M_f(hf_i^A), y_f^i) \quad (9)$$

where CE is the Cross-Entropy loss comparing the prediction with the ground-truth node type label  $y_f^i$ .

The final pre-training loss  $\mathcal{L}_p$  is a weighted combination of these two task-specific losses:

$$\mathcal{L}_p = \alpha \mathcal{L}_s + \beta \mathcal{L}_f \quad (10)$$

where  $\alpha$  and  $\beta$  are scalar hyperparameters that balance the relative importance of the structural and functional pre-training tasks.

### 3.6 Downstream Tasks

As shown in Fig 3, for the downstream task, we train a classifier to predict the post-mapping delay characteristics of each cut  $C$ , which then guides the mapping engine. The ground-truth post-mapping delay  $dc$  for a cut is first discretized into  $K$  classes. Our research indicates that the distribution of cell delays is mainly concentrated below 500 ps. As illustrated in Fig 4, we extract cell delays from the post-mapping netlists of 5 randomly chosen combinational circuits; results show that most of these cell delays are under 500 ps. We use  $K = 8$  classes (e.g., Class 0 for 0–100 ps, Class 1 for 100–200 ps, ..., and Class 7 for >700 ps). This binning process creates a ground-truth label  $y_C$  for each cut.

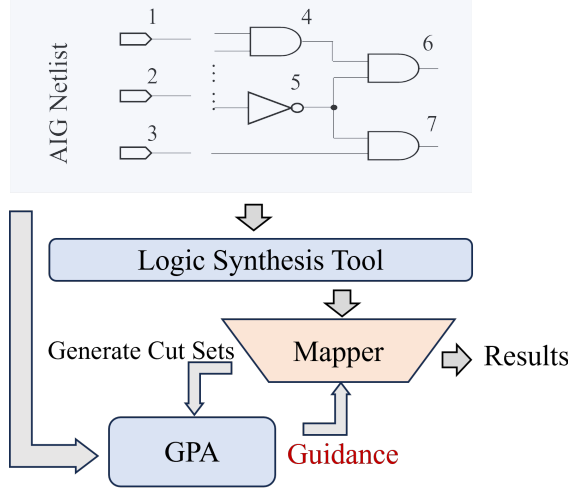


**Figure 3: Work Flow of the proposed framework:** First, the technology-independent AIG netlist is input into the logic synthesis tool to generate candidate cut sets. Then, the pre-trained GPA model performs inference on these cuts to predict their post-mapping delay classes. Finally, these predictions serve as guidance (cost metric) for the mapper’s dynamic programming algorithm to select the optimal cuts, yielding the final technology-mapped results.

A final classifier  $M_d$ , typically an MLP, takes the learned cut embedding  $e_C$  (and optionally the global technology embedding  $e_p$ ) to predict the delay class  $\hat{y}_C$ :

$$\hat{y}_C = M_d(\text{cat}(e_C, e_p)) \quad (11)$$

The model is then fine-tuned on this task by minimizing a classification loss, typically the Cross-Entropy (CE) loss  $\mathcal{L}_d$ :

$$\mathcal{L}_d = \sum_{C \in C_{\text{train}}} \text{CE}(\hat{y}_C, y_C) \quad (12)$$

where  $C_{\text{train}}$  is the set of candidate cuts in the training data.

In practice, we integrate this trained GPA model into a logic synthesis tool (e.g., ALSO). The mapper generates candidate cuts, GPA performs inference to assign a predicted delay class  $\hat{y}_C$  to each. This class is then used as the cost metric for the mapper’s dynamic programming algorithm to select the final, delay-optimal cover.

## 4 Experiments

### 4.1 Experiment Settings

**4.1.1 Data Preparation.** Our training datasets are sourced from ForgeEDA [25] and DeepCircuitX [26], which aggregate open-source repository-level designs from GitHub. The AIG encoder, PM encoder, and transformer are pre-trained on 15,000 randomly selected sub-circuits, with sizes up to 4096 nodes, to enable efficient model pre-training.

For model training and validation, we employ the open-source technology library *Sky130nm* [27], *Asap7nm* [28] and the open-source logic synthesis tool ALSO primarily built on morkturtle to generate post-mapping netlists. To extract training labels for each

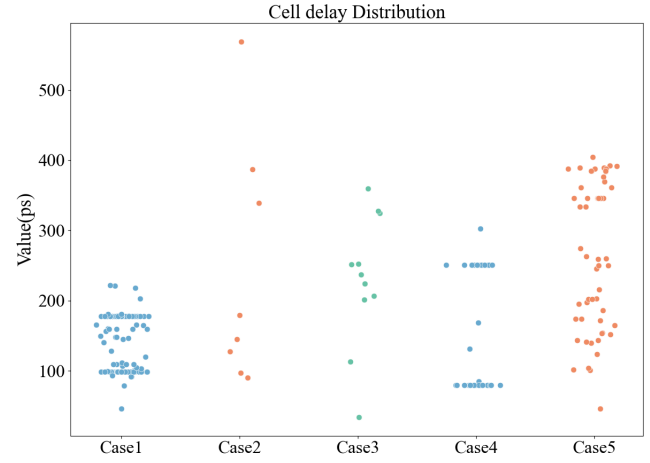


**Figure 4: Cell delay distribution**

implemented node cut along the critical path, we first map AIG format circuits to post-mapping netlists using command "techmap -o" [10] for technology mapping or "mch -M 0 -S -l 49 -o" [2] for mixed structure choice mapping, and generate the corresponding Verilog files. We then extract the critical path via the ABC [29] command "stime -p" to obtain gate types and their respective delays from the post-mapping netlists in a topo-order. When an inverter is inserted into a cell on the critical path, the inverter’s delay will be incorporated into the cell’s total delay, as they are regarded as a single integrated entity. The total training dataset includes 5000 randomly selected sub-circuits from ForgeEDA and DeepCircuitX.

To collect corresponding cuts in AIG netlists, we output the implemented cuts in the final cover and apply a backtracking algorithm to identify relevant cuts according to gates generated from critical path. Using this approach, the cuts can be trained using real path delays, along with efficient path and functional information.

**4.1.2 Evaluation Metrics.** To validate the rationality of this cut embedding generation in GPA and its ability to effectively identify the delay classes of cells, we utilize accuracy to demonstrate and validation loss to avoid overfitting.

The cut classification loss ( $\mathcal{L}_{\text{cut}}$ ), which we refer to as the transformer pooling loss, is defined using the Cross-Entropy (CE) loss. It is calculated over the set of candidate cuts  $C$ :

$$\mathcal{L}_{\text{cut}} = \sum_{c \in C} \text{CE}(\text{MLP}(e_c), y_c) \quad (13)$$

where  $e_c$  is the final embedding for cut  $c$  generated by the transformer and pooling module, MLP is the final classifier head that predicts the delay class, and  $y_c$  is the ground-truth delay class label for cut  $c$ , derived from post-mapping critical path analysis.

The accuracy is calculated as the fraction of correctly predicted cut classes:

$$\text{Accuracy} = \frac{1}{|C|} \sum_{c \in C} \mathbb{I}(\text{argmax}(\text{MLP}(e_c)) == y_c) \quad (14)$$

where  $|C|$  is the total number of cuts in the evaluation set,  $\mathbb{I}$  is the indicator function (1 if the condition is true, 0 otherwise), and  $\text{argmax}(\text{MLP}(e_c))$  is the model’s predicted delay class for cut  $c$ .

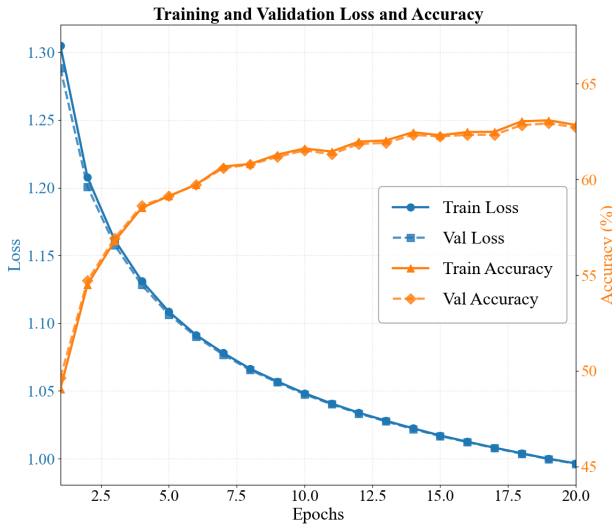


Figure 5: Training process of GPA

As shown in Fig. 5, We train GPA for 20 epochs until the accuracy plateaued. With a final accuracy exceeding 60%, this demonstrates that the model can effectively learn the delay of matched cuts via its leaf nodes, thereby validating our assertion.

**4.1.3 Training and Model implementation.** The Transformer-based model employed to refine AIG node embeddings comprises 4 Transformer blocks, each with 8 attention heads. After encoding, each AIG node is represented as a 128-dimensional structural embedding paired with a 128-dimensional functional embedding. AIG encoder and PM encoder undergoes pretraining for 60 epochs in Stage 1, followed by an additional 60 epochs in Stage 2, to ensure convergence. The pretraining process uses a batch size of 32 and is performed on one Nvidia A800 GPU. For optimization, we use the Adam optimizer with a learning rate of  $10^{-4}$ .

## 4.2 Experimental Results

**4.2.1 Comparison with traditional algorithm.** We integrate GPA into ALSO, an open-source logic synthesis framework based on mockturtle, and evaluate it on the EPFL combinational benchmark

suite using the *SkyWater 130nm* library. Compared to the baseline “techmap” flow, GPA achieves an average 19.9% delay reduction with a manageable 25% area overhead. As shown in Table 4, 14 out of 19 benchmarks show improved delay, with particularly strong gains—up to 65% reduction—on critical circuits like “adder”. These results demonstrate GPA’s effectiveness in guiding mapping decisions through accurate, path-aware delay prediction.

To further demonstrate GPA’s versatility and scalability in mixed-structure circuits, we replace the AIG encoder with a pretrained XOR-Majority Graph (XMG) encoder, enabling GPA to natively leverage heterogeneous logic representations. Evaluated across the same 19 EPFL benchmarks under the *SkyWater 130nm* library, GPA with XMG outperforms the state-of-the-art mixed-structure operator MCH—reducing delay in 13 of 19 circuits, with an average

gain of 2.1% and a peak reduction of 19.1% on the “max” benchmark. Remarkably, this improvement is accompanied by a 2.4% area reduction across all benchmarks—contrary to conventional trade-offs—revealing that structure-aware, data-driven learning not only enhances timing but also enables simultaneous area optimization. These results expose the inherent rigidity of traditional structural heuristics and underscore GPA’s unique ability to learn optimal structural composition from data, rather than enforce fixed rules.

**4.2.2 Comparison with ML-based method.** To highlight the importance of functional semantics and path-aware delay modeling, we compare GPA against the prior state-of-the-art framework SLAP. Using SLAP’s open-source implementation and its `./abc-train` flow under the *ASAP 7nm* library, we reproduce its results on the 19 EPFL benchmarks. For fair comparison, we retrain GPA on the same *ASAP 7nm*-mapped circuits. Results show that GPA achieves an average 4.1% delay reduction over SLAP across all benchmarks, with 10 out of 19 circuits showing improved performance. Notably, the “dec” benchmark sees a dramatic 69.3% delay improvement, underscoring GPA’s superior generalization. We attribute this gain to GPA’s ability to jointly embed circuit functionality and path-dependent timing context—enabling more accurate cut selection than SLAP’s handcrafted feature-based approach.

## 5 Conclusion

Our approach tackles the inaccurate delay estimation limitation in traditional technology mapping via GPA, a GNN-based path-aware multi-view circuit learning model. Its core innovation lies in capturing comprehensive circuit information (functional characteristics, target technology attributes) through the synergistic integration of AIG encoding, PM encoding, and path-aware Transformer pooling. Trained on real post-mapping critical path delays, GPA delivers accurate delay class predictions for candidate cuts, enabling mapping engines to select optimal cuts based on realistic delay costs.

Future work will focus on expanding GPA’s ability to predict more cell delay classes and improving prediction accuracy, requiring additional modules to connect technology-independent logic networks with gate-level netlists and integrating more post-mapping information affecting cell delay.

**Table 1: Technology Mapping Performance Comparison between w/ GPA and w/o GPA on EPFL Benchmark Suite**

Benchmarks	Skywater 130nm								Asap 7nm	
	techmap [10] w/o ours		mch [2] w/o ours		techmap w/ ours		mch w/ ours		SLAP [5]	ours
	area	delay	area	delay	area	delay	area	delay	delay	delay
adder	4444.3	49100.6	4306.6	17366.1	4464.3	<b>16866.9</b>	3970.1	20982.7	2049.9	3905.7
bar	14940.6	4780.7	14796.7	5369.2	12864.8	5074.3	11240.8	<b>4717.0</b>	1181.5	<b>660.7</b>
div	215236.4	500865.9	218010.3	554782.4	256154.4	<b>420589.2</b>	212867.9	581811.7	78853.6	82933.0
log2	94590.7	60953.6	94132.8	61156.3	125990.8	<b>45529.6</b>	92892.8	<b>57060.3</b>	8903.9	<b>6450.6</b>
max	10105.9	40425.7	9960.8	46248.0	13431.6	<b>32754.4</b>	9824.4	<b>37430.0</b>	5145.4	<b>2300.9</b>
multiplier	78361.4	45314.6	80843.8	37932.4	104856.8	<b>26330.9</b>	80120.6	<b>36861.0</b>	4824.8	<b>4458.7</b>
sin	18743.0	28179.8	18701.7	24751.1	22636.7	<b>21676.6</b>	18242.5	<b>24168.9</b>	4104.8	<b>3243.8</b>
sqrt	91220.0	1349133.8	86192.7	993878.3	113861.7	<b>657474.4</b>	91951.9	<b>833586.3</b>	309490.3	<b>141313.1</b>
square	62762.7	29421.5	63565.0	22631.7	78480.3	<b>17700.4</b>	63109.3	<b>21423.2</b>	2457.0	3962.4
arbiter	32881.5	6768.6	32986.6	6690.9	45562.5	7623.7	32406.1	7791.5	723.4	1392.8
cavlc	2128.3	1674.3	2167.1	1555.8	3040.4	<b>1632.0</b>	2120.8	<b>1399.2</b>	242.8	<b>230.8</b>
dec	1273.7	831.2	1273.7	831.1	1171.1	<b>583.8</b>	1191.1	<b>621.8</b>	368.6	<b>113.3</b>
i2c	4317.9	1585.9	4396.7	2139.1	6020.7	<b>1503.8</b>	4362.9	<b>1865.5</b>	234.8	244.4
int2float	721.9	1277.3	710.7	1185.7	1106.1	<b>1224.1</b>	734.5	1399.2	114.6	160.4
mem_ctrl	143943.1	18253.8	145642.2	22668.5	201200.5	19672.1	147585.3	<b>20431.2</b>	6129.4	<b>3337.1</b>
router	975.9	3994.5	962.2	3695.1	1143.6	4291.5	929.6	4637.9	345.1	762.4
priority	3275.6	18771.3	3256.9	18686.6	4356.7	<b>14089.0</b>	3318.2	<b>17896.5</b>	1772.7	2820.6
voter	50637.3	7896.7	50048.0	7993.9	64159.0	<b>7613.4</b>	48225.0	<b>7602.0</b>	1150.4	<b>1052.1</b>
ctrl	464.2	807.5	424.2	677.6	649.4	830.6	444.2	867.9	81.4	130.3
GEOMEAN	12049.1	13356.8	11954.9	12376.8	15057.0	10695.2	11670.1	12122.3	1812.3	1737.3
Ratio	1	1	1	1	1.250	<b>0.801</b>	<b>0.976</b>	<b>0.979</b>	1	<b>0.959</b>

## References

- [1] Satrajit Chatterjee, Alan Mishchenko, Robert K Brayton, Xinning Wang, and Timothy Kam. Reducing structural bias in technology mapping. *IEEE Transactions on Computer-Aided Design of Integrated Circuits and Systems*, 25(12):2894–2903, 2006.
- [2] Zhang Hu, Hongyang Pan, Yinshui Xia, Lunyao Wang, and Zhufei Chu. Mixed structural choice operator: Enhancing technology mapping with heterogeneous representations. In *2025 62nd ACM/IEEE Design Automation Conference (DAC)*. IEEE, 2025.
- [3] Luca Amaru, Pierre-Emmanuel Gaillardon, and Giovanni De Micheli. Majority-inverter graph: A new paradigm for logic optimization. *IEEE Transactions on Computer-Aided Design of Integrated Circuits and Systems*, 35(5):806–819, 2015.
- [4] Rajendran Panda and Farid N Najm. Post-mapping transformations for low-power synthesis. *VLSI Design*, 7(3):289–301, 1998.
- [5] Walter Lau Neto, Matheus T Moreira, Yingjie Li, Luca Amaru, Cunxi Yu, and Pierre-Emmanuel Gaillardon. Slap: A supervised learning approach for priority cuts technology mapping. In *2021 58th ACM/IEEE Design Automation Conference (DAC)*, pages 859–864. IEEE, 2021.
- [6] Chandrabhusan Reddy Chigarapally, Harshwardhan Nitin Bhakkad, Animesh Basak Chowdhury, Chandan Karfa, and Sukanta Bhattacharjee. Leap: Learning guided quality cut selection for faster technology mapping. In *Proceedings of the 43rd IEEE/ACM International Conference on Computer-Aided Design*, pages 1–6, 2024.
- [7] Junfeng Liu, Liwei Ni, Xingquan Li, Min Zhou, Lei Chen, Xing Li, Qinghua Zhao, and Shuai Ma. Aimap: Learning to improve technology mapping for asics via delay prediction. In *2023 IEEE 41st International Conference on Computer Design (ICCD)*, pages 344–347. IEEE, 2023.
- [8] Zhengyuan Shi, Hongyang Pan, Sadaf Khan, Min Li, Yi Liu, Junhua Huang, Hui-Ling Zhen, Mingxuan Yuan, Zhufei Chu, and Qiang Xu. Deepgate2: Functionality-aware circuit representation learning. In *2023 IEEE/ACM International Conference on Computer Aided Design (ICCAD)*, pages 1–9. IEEE, 2023.
- [9] Zhengyuan Shi, Chengyu Ma, Ziyang Zheng, Lingfeng Zhou, Hongyang Pan, Wentao Jiang, Fan Yang, Xiaoyan Yang, Zhufei Chu, and Qiang Xu. Deepcell: Multiview representation learning for post-mapping netlists. *arXiv preprint arXiv:2502.06816*, 2025.
- [10] Alessandro Tempia Calvino, Heinz Riener, Shubham Rai, Akash Kumar, and Giovanni De Micheli. A versatile mapping approach for technology mapping and graph optimization. In *ASP-DAC*, pages 410–416, 2022.
- [11] Min Li, Sadaf Khan, Zhengyuan Shi, Naixing Wang, Huang Yu, and Qiang Xu. Deepgate: Learning neural representations of logic gates. In *Proceedings of the 59th ACM/IEEE Design Automation Conference*, pages 667–672, 2022.
- [12] Zhengyuan Shi, Min Li, Sadaf Khan, Liuzheng Wang, Naixing Wang, Yu Huang, and Qiang Xu. Deeppti: Test point insertion with deep reinforcement learning. In *2022 IEEE International Test Conference (ITC)*, pages 194–203. IEEE, 2022.
- [13] Haonan Wei, Wentao Jiang, Zhang Hu, Zhengyuan Shi, Yinshui Xia, Lunyao Wang, and Zhufei Chu. Auto-cec: Combinational equivalence checking via intelligent sweeping engine selection. In *2025 International Symposium of Electronics Design Automation (ISED)*, pages 449–454. IEEE, 2025.
- [14] Zhengyuan Shi, Ziyang Zheng, Sadaf Khan, Jianyuan Zhong, Min Li, and Qiang Xu. Deepgate3: Towards scalable circuit representation learning. In *Proceedings of the 43rd IEEE/ACM International Conference on Computer-Aided Design*, pages 1–9, 2024.
- [15] Ziyang Zheng, Shan Huang, Jianyuan Zhong, Zhengyuan Shi, Guohao Dai, Ningyi Xu, and Qiang Xu. Deepgate4: Efficient and effective representation learning for circuit design at scale. *arXiv preprint arXiv:2502.01681*, 2025.
- [16] Chenhui Deng, Zichao Yue, Cunxi Yu, Gokce Sarar, Ryan Carey, Rajeev Jain, and Zhiru Zhang. Less is more: Hop-wise graph attention for scalable and generalizable learning on circuits. In *Proceedings of the 61st ACM/IEEE Design Automation Conference*, pages 1–6, 2024.
- [17] Jiawei Liu, Jianwang Zhai, Mingyu Zhao, Zhe Lin, Bei Yu, and Chuan Shi. Polargate: Breaking the functionality representation bottleneck of and-inverter graph neural network. In *Proceedings of the 43rd IEEE/ACM International Conference on Computer-Aided Design*, pages 1–9, 2024.
- [18] Zhengyuan Shi, Jingxin Wang, Wentao Jiang, Chengyu Ma, Ziyang Zheng, Zhufei Chu, Weikang Qian, and Qiang Xu. Alignment unlocks complementarity: A framework for multiview circuit representation learning, 2025.
- [19] Jingxin Wang, Renxiang Guan, Kainan Gao, Zihao Li, Hao Li, Xianju Li, and Chang Tang. Multi-level graph subspace contrastive learning for hyperspectral image clustering. In *2024 International Joint Conference on Neural Networks (IJCNN)*, pages 1–8. IEEE, 2024.
- [20] Xufeng Yao, Yiwen Wang, Xing Li, Yingzhao Lian, Ran Chen, Lei Chen, Mingxuan Yuan, Hong Xu, and Bei Yu. Rtlrewriter: Methodologies for large models aided rtl code optimization. In *Proceedings of the 43rd IEEE/ACM International Conference on Computer-Aided Design*, pages 1–7, 2024.
- [21] Wenji Fang, Shang Liu, Jing Wang, and Zhiyao Xie. Circuitfusion: multimodal circuit representation learning for agile chip design. *arXiv preprint arXiv:2505.02168*, 2025.
- [22] Karunakar R Basirreddy, Srinivas Sabbavarapu, and Amit Acharyya. Cut-less technology mapping using shannon factor graph with on-the-fly size reduction. *Journal of Low Power Electronics*, 14(3):448–457, 2018.
- [23] Zhang Hu, Chengyu Ma, and Zhufei Chu. A novel structural choices generation method for logic restructuring. In *2024 2nd International Symposium of Electronics Design Automation (ISED)*, pages 306–311. IEEE, 2024.
- [24] Mathias Soeken, Luca Gaetano Amaru, Pierre-Emmanuel Gaillardon, and Giovanni De Micheli. Exact synthesis of majority-inverter graphs and its applications. *IEEE Transactions on Computer-Aided Design of Integrated Circuits and Systems*, 36(11):1842–1855, 2017.
- [25] Zhengyuan Shi, Zeju Li, Chengyu Ma, Yunhao Zhou, Ziyang Zheng, Jiawei Liu, Hongyang Pan, Lingfeng Zhou, Kezhi Li, Jiaying Zhu, et al. Forgedea: A comprehensive multimodal dataset for advancing eda. *arXiv preprint arXiv:2505.02016*, 2025.
- [26] Zeju Li, Changran Xu, Zhengyuan Shi, Zedong Peng, Yi Liu, Yunhao Zhou, Lingfeng Zhou, Chengyu Ma, Jianyuan Zhong, Xi Wang, et al. Deepcircuitx: A comprehensive repository-level dataset for rtl code understanding, generation, and ppa analysis. *arXiv preprint arXiv:2502.18297*, 2025.
- [27] Google. Skywater open source pdk. 2020.
- [28] Lawrence T Clark, Vinay Vashishtha, Lucian Shifren, Aditya Gujja, Saurabh Sinha, Brian Cline, Chandrasekaran Ramamurthy, and Greg Yeric. Asap7: A 7-nm finfet predictive process design kit. *Microelectronics Journal*, 53:105–115, 2016.
- [29] Robert Brayton and Alan Mishchenko. Abc: An academic industrial-strength verification tool. In *International Conference on Computer Aided Verification*, pages 24–40. Springer, 2010.